

One Step Annealing Treatment for Performance Improvement of Silicon Anode Based on Polyimide Binder

Li Zhu, Haoqing Hou^{*}, Dan Zhao, Shuwu Liu, Wan Ye, Shuliang Chen and Muddasir Hanif

Department of Chemistry and Chemical Engineering, Jiangxi Normal University, 330022, Nanchang, China

^{*}E-mail: hhq2001911@126.com

Received: 18 July 2015 / Accepted: 2 September 2015 / Published: 30 September 2015

Li-ion batteries have many industrial applications. We report a one step annealing treatment of the silicon anode for Li-ion battery to improve the electrochemical performance and stability. We have used a polyimide (PI) with high mechanical strength and excellent thermal stability as a polymeric binder to get better performance. The physical properties of the PI binder improved the surface morphology, lithiation and delithiation process. The Si anode shows a high initial charge reversible capacity of 1195.6 mAh g⁻¹ and charge capacity retention of 93.6% for 30 cycles. Based on AFM image, cyclic voltammetry, electrochemical impedance spectroscopy and SEM image, we conclude that the annealed anode has much better charge reversible capacity in comparison to the non-annealed anode. These improvements are attributed to the compact surface morphology of the silicon electrode reconstructed by the PI binder and annealing treatment. The annealing temperature plays an important role to improve the performance of Si anode.

Keywords: Li-ion batteries; polyimide binder; silicon anode; annealing treatment

1. INTRODUCTION

Rechargeable Li-ion batteries have been extensively developed in various commercial fields, for example, personal electronics, defense, aerospace, power tools and transportation and so on. In recent years, silicon has attracted considerable attention because it has an extremely high theoretical capacity of 4200 mAh g⁻¹ and relatively low potential for Li ion insertion [1]. However, the low electrical conductivity of silicon material and the volume expansion during the repeated insertion and extraction of lithium are the two major problems for Si-based anodes in Li-ion batteries [2-3].

Important and attractive strategies to address these issues include the control of Si surface morphologies, such as Si nanowires [4], Si nanotubes [5], Si thin films [6] and Si hollow nanospheres

[7]. They show good electrochemical performance because all kinds of structures can adapt to Si volume changes upon lithium insertion. Another approach is forming Si/C composites. Silicon based composites consist of silicon and a pyrolyzed carbon coating. Polyvinylidene fluoride [8], polyaniline [9], polyvinyl chloride [10], phenolic resin [11] have been usually used as carbon coating precursors. Silicon based composites are effective to enhance conductivity of Si and then buffer the volume changes of silicon during repeated lithiation and delithiation cycles. In addition, commercial polyvinylidene fluoride (PVdF) binder is not abundant to fit the enormous volume changes (around 300%) in silicon based material. Therefore, the choice of the binder is very important to improve the electrochemical performance of Si anode. The commonly used binders are by far polyacrylic acid (PAA) [12], sodium carboxymethyl cellulose [13], polyamide imide (PAI) [14], polyimide (PI) [15], and even some self healing polymers [16]. Kim et al. shows that the surface of silicon is modified by Ag-assisted chemical etching process and the silicon anodes using PI as a binder shows the charge capacity retention of 75.9% after 20 cycles [17]. Moreover, the etched Si-PI electrode shows poor cycle performances.

In this manuscript, we propose an innovative thermally polyimide (PI) as binder and the use of one step annealing treatment following the slurry casting for silicon-based electrodes. To our knowledge, PI is an important engineering plastic with good mechanical and thermal properties. Morphology of the silicon electrode is reconstructed after annealing treatment. The compact morphology will not only hinder Si volume changes to some extent, but also improve specific capacity of silicon anode. Both of those common functions improve silicon anode stability and other attractive attributes. Therefore, the annealed (300 °C) silicon electrode and PI as binder exhibits a high reversible capacity of 1195.6 mAh g⁻¹ at a 0.1 C current density and charge capacity retention of 93.6% for 30 cycles.

2. EXPERIMENTAL

2.1 Cell fabrication

For the electrochemical tests, a slurry was produced by mixing nano silicon particles as an active material (50 wt. %), carbon black (CB) and acetylene black (AB) (w:w=1:1) as an electronic conducting agent (30, 25, 20 wt.%) and PI as the binder (20, 25, 30 wt.%) dissolved in an anhydrous *N*-methyl-2-pyrrolidinone (NMP). The obtained slurry was coated on a copper foil, and then the composite electrode was dried at 100 °C under vacuum for 12 h. The lower content of silicon and high content of carbon makes for the improvement electric conductivity of silicon anode. The electrode material loading was 0.5~0.54 mg cm⁻² (including Si, AB & CB and PI). Some electrodes further processed by an annealing treatment at different temperatures under nitrogen gas for 20 min.

LIR 2032 coin-type half cells were assembled and sealed in an Ar-filled glove box (H₂O < 1 ppm, O₂ < 1 ppm). The electrolyte solution comprised of 1 M lithium hexafluoro phosphate (LiPF₆) in a mixture of ethylene carbonate (EC) and dimethyl carbonate (DMC) and ethyl methyl carbonate (EMC) at a 1:1:1 volume ratio. The Si electrode acted as working electrode and lithium metal foil as the

counter electrode. The three layer microporous composite membranes (polypropylene, polyethylene and polypropylene (PP/PE/PP)) were used as a separator.

2.2 Characterization

The material morphology was examined with a scanning electronic microscopy (SEM, VEGA 3 SBU) operating at 2 kV and atomic force microscopy (AFM, MicroNano). Cyclic voltammetry (CV) and electrochemical impedance spectroscopy (EIS) were monitored by means of Bio-Logic VMP3-based instruments. CV of 2032 coin-type half cells was measured at the scan rate of 0.05 mV s^{-1} in the potential window of 0.01~1.5 V. Cell impedances were performed over a frequency range of 10 mHz to 0.1 MHz and a applied amplitude voltage of 5 mV after five cycles. Galvanostatic charge and discharge cycling tests (LAND CT2001A battery measurement system) were performed in the potential window from 10 mV to 1.5 V vsersus Li/Li^+ at a 0.1 C (1C equal to the sum of the theoretical specific capacity of silicon content and carbon content) rate. All measurements are performed at room temperature. In this paper, the alloying process of Si with Li and the dealloying are regarded as the discharge process and the charge process, separately. The total weight of silicon, carbon black (CB) and acetylene black (AB) and polyimide (PI) were used to compute the capacities of silicon electrode.

3. RESULTS AND DISCUSSION

3.1 The effect of binder contents and annealed temperatures

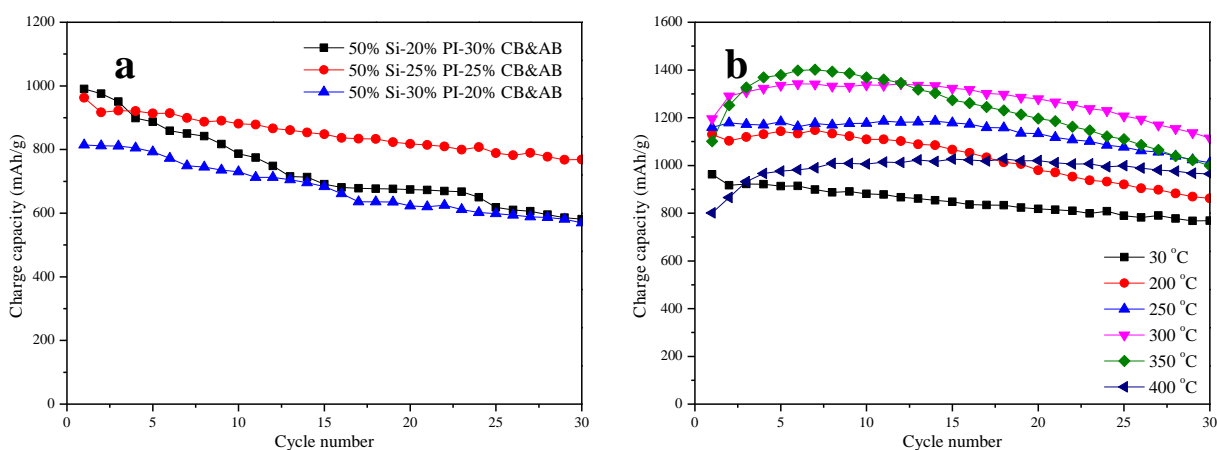


Figure 1. The cycle performance of silicon electrodes (a) with different binder contents and (b) annealed for 20 min at different temperatures

Ding et al. have proved that silicon anode with small content of silicon and large content of binder can enhance the cycle performance to a certain degree [18]. However, a great deal of binder may hinder the paths of lithium ion intercalation silicon anode. Therefore, the ratio of silicon contents to non-active substance (containing binder and conductive additive) contents has to be 1 to 1. The effect of binder contents of 20%, 25% and 30% were investigated. As shown in Fig. 1(a), the charge

capacities were increased and then decreased as the binder amount is increased. Stable reversible capacities of 990.3, 963 and 814.1 mAh g⁻¹ were observed for the electrodes with 20% PI, 25% PI and 30% PI, respectively. Moreover, the cyclability of silicon anode with 50% Si-25% PI-25% CB&AB are better than the silicon anode with other proportions of PI.

Fig. 1(b) presents the cycle performance of the silicon anode with 50% Si-25% PI-25% CB&AB annealed for 20min at different temperatures. We can observe that charge capacities have increased and then decreased as the annealing temperatures were varied from 30 to 400 °C. All the annealed electrodes showed much better charge capacities than the non annealed electrodes. The charge capacity of 862.1, 1011.5, 1114.5, 999 and 964.9 mAh g⁻¹ for 30 cycles were observed for annealed electrodes, annealed at 200 °C, 250 °C, 300 °C, 350 °C and 400 °C, respectively. These results confirm that the silicon anode annealed at 300 °C show much better stability than the electrodes annealed at other temperatures. The capacities of silicon anode with annealing treatment gradually increased for the first 5 cycles. As reported by the Magasinski et al., the capacities increased after the first cycle because of silicon electrode step by step activity process [12].

3.2 AFM Analysis

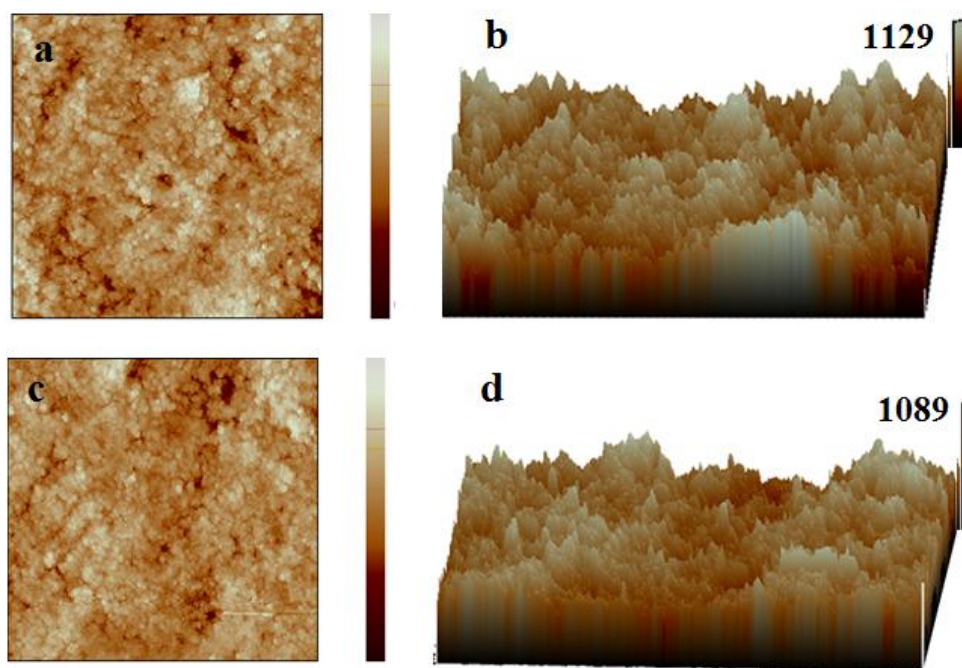


Figure 2. AFM images of silicon anode: (a) the non annealing treatment; (b) 3D of the non annealing treatment; (c) the annealing treatment; (d) 3D of the annealing treatment

Fig. 2(a) and 2(c) display (AFM image) the surface morphology of silicon anode without and with annealing treatment, respectively. The non-annealed silicon anode shows a microporous structure. Most nano-silicon particles are exposed and isolated without interconnection. The annealing treatment is performed above the glass transition temperature of PI (230 °C). This induces the molecular movement of PI chain, which fills the gaps between nano-Si particles and allows the reconstruction of

surface morphology of silicon anode. Therefore, surface of the annealed silicon anode becomes more compact and flat than the non-annealed anode. Fig. 2(b) and 2(d) shows separately the three-dimensional (3D) figures of Fig. 2(a) and 2(c). From these figures, we obtained the heights, 1129 and 1089 nm, respectively, which reveals that the surface of the annealed electrode is comparatively more uniform.

3.3 Electrochemical Characteristics

3.3.1 The cycle performance of silicon anode

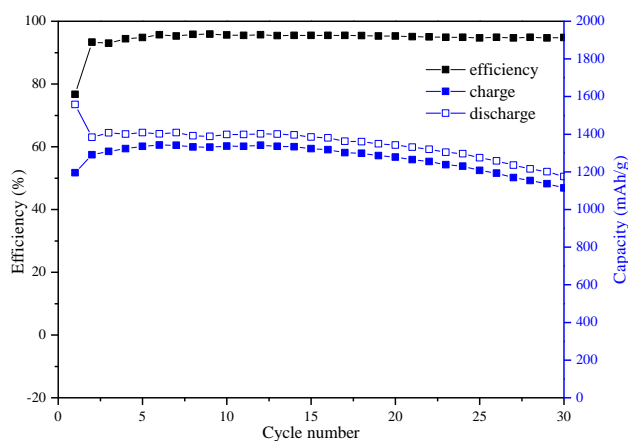


Figure 3. The cycle performance and coulombic efficiency of annealed silicon anode by 300 °C treatment

Fig. 3 shows the cycle performance and coulombic efficiency of the silicon anode annealed at 300 °C. As is seen, the silicon anode annealed at 300 °C shows charge capacity and discharge capacity of 1195.6 and 1558 mAh g⁻¹, respectively, and coulombic efficiency of 76.7% in the first cycle. After 30 cycles, the annealed anode still shows a stable reversible capacity of 1114.5 mAh g⁻¹ and charge capacity retention of 93.6%. However, the stable reversible capacity and charge capacity retention of the non-annealed anode for 30 cycles is 768.3 mAh g⁻¹ and 79.8%, separately, as shown in Fig. 1. The result reveals that the annealed anode has much better reversible capacity than the non-annealed silicon anode.

3.3.2 The charge-discharge studies

Lithium ion intercalate into silicon anode in the discharge process, however it cannot deintercalate completely in the charge process. This causes the formation of irreversible capacity, especially in the initial cycles. The interface reaction between active material and LiPF₆-based electrolyte leads to the irreversible capacity, which is the occurrence of solid electrolyte interface (SEI)

[19]. Furthermore the Li ion storage at the surface, holes and cracks of the electrode is a critical way for the formation of irreversible capacity [20].

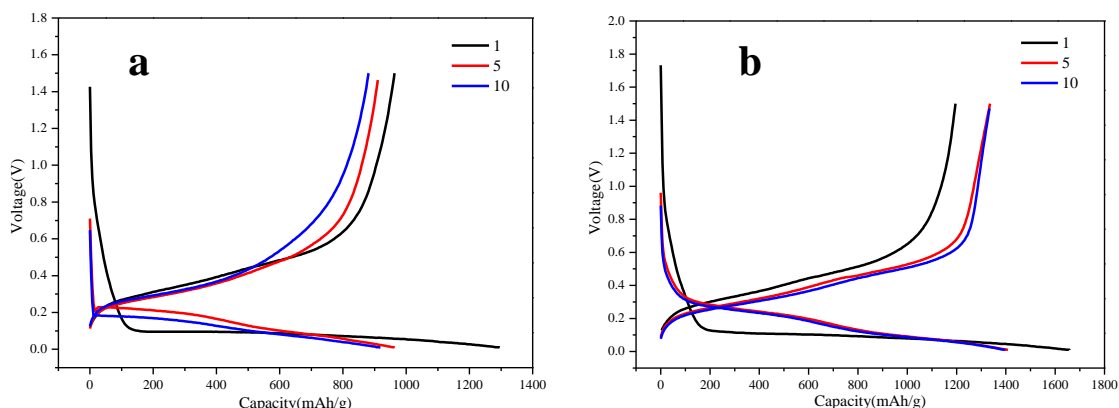


Figure 4. Charge-discharge curves of silicon anode with and without annealing treatment

As shown in Fig. 4, a long flat plateau about at 0.1 V may be related to the Li ion intercalation into silicon anode and the formation of Li-Si alloys in the first discharge process. The profile of the first charge shows the sloping plateau between 0.2 V and 0.8 V, representative of the de-alloying process [21, 22]. The result is consistent with the CV curves. Capacity change mainly appears at the plateau, longer the voltage plateau is, higher is the capacity. Therefore, charge and discharge capacity of the annealed anode is higher than the non-annealed anode. It reveals that the capacity of silicon anode is improved after annealing treatment. As demonstrated in the Fig. 4(b), the capacity of the annealed anode increase gradually in the first 10 cycles, indicating that some of the nano silicon particles were not originally active. The initially inactive Si nanoparticles likely expose to the electrolyte in the late lithium insertion and extraction process. In comparison, the capacity of the non-annealed silicon anode is significantly lower and decreases gradually.

3.3.3 CV studies

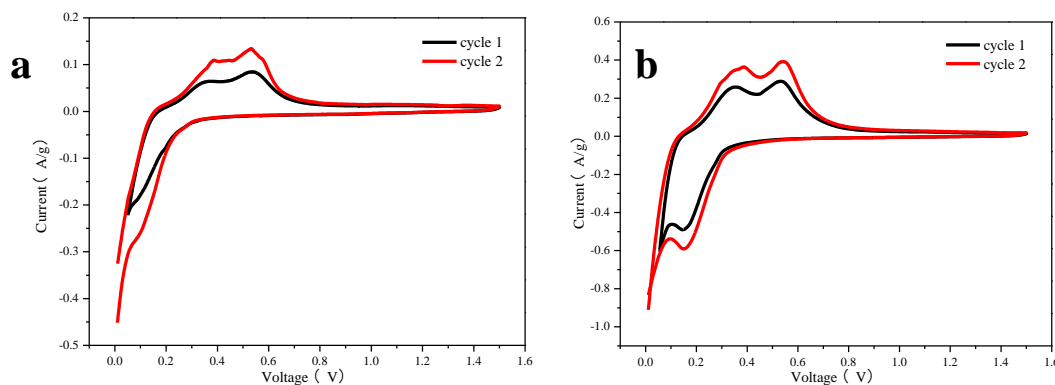


Figure 5. Cyclic voltamogram of silicon anode: a) anode without annealing process before cycles; b) anode with annealing process before cycles

Fig. 5 shows the cyclic voltammetry (CV) curves of the silicon anode with and without annealing. For the annealed silicon anode (Fig. 5(b)), the peak starting at ~ 0.15 V in the first cathodic scan corresponds to the Li-ion intercalation into Si to the formation of Li_xSi phase. The two peaks at ~ 0.35 and 0.54 V in the first anodic scan correspond to Li-ion extraction from the Li_xSi phase, which is in agreement with the previous reports [23-25]. However, as can be seen from Fig. 5(a), the non-annealed silicon electrode does not show clear peak at ~ 0.15 V, which demonstrates having lower electrochemical activity of lithium insertion. After several cycles, the intensity of the peaks (current density) increases. This reveals that more Si nanoparticles are reacting with Li-ion and the silicon electrode is gradually active. The cycle performance of silicon electrode is increased. Although the non-annealed Si electrode has similar peak potential, the intensity of the peak (current density) has big difference from the annealed Si electrode. This reveals that the annealed silicon electrode has higher electrochemical activity.

3.3.4 EIS studies

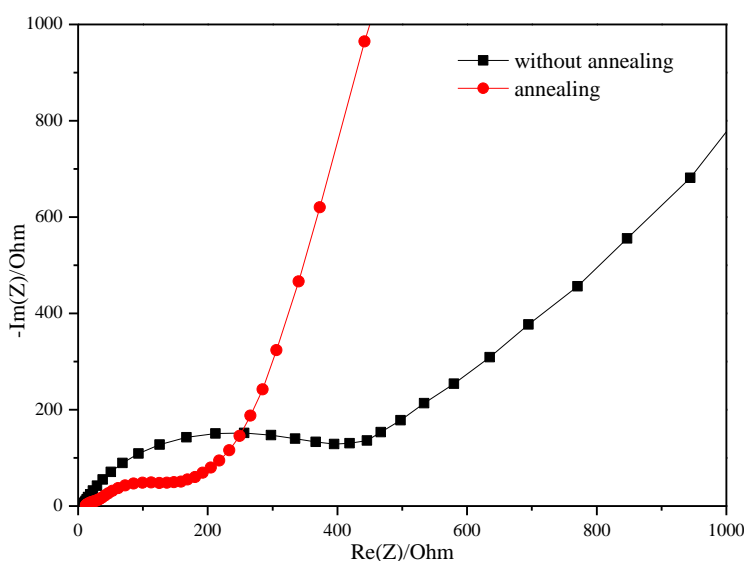


Figure 6. EIS of silicon anode with/without annealing treatment (at delithiation state)

The kinetics of Li-ions intercalation and de-intercalation with the silicon electrode was further studied by the EIS measurements. Fig. 6 compares the Nyquist plots of the annealed electrode and the non annealed electrode after 5 cycles. It is well-known that the semicircles in the high frequency region is related to the real charge transfer resistance, whereas the straight line in the low frequency region reflect the Warburg diffusion of lithium ions for silicon electrodes [26, 27]. As shown in Fig. 6, the real charge transfer resistance of the annealed anode is reduced remarkably, indicating that the electron transmission speed increased as compared with the non annealed electrode. In other words, the conductivity of the electrode has improved dramatically after the annealing treatment.

3.4 Morphology characterization

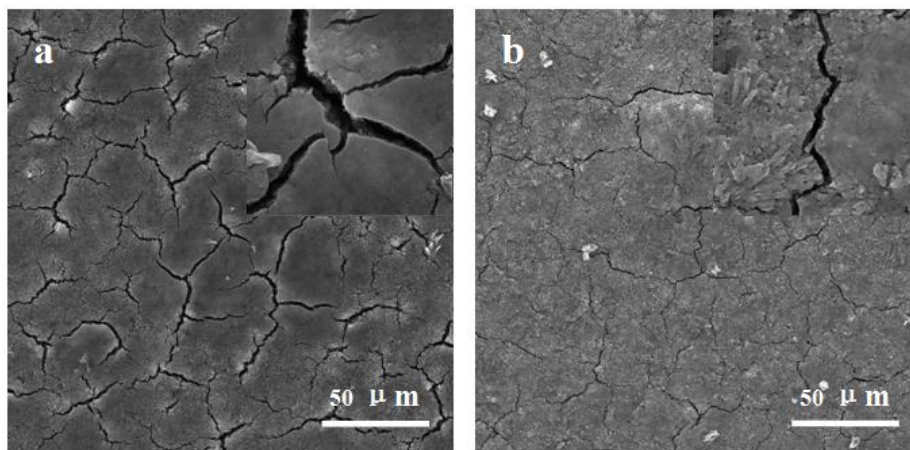


Figure 7. SEM images of anode electrodes: (a) cycled electrode without annealing treatment; (b) cycled electrode with annealing treatment.

The Fig. 7 shows the morphologies of Si electrodes with and without annealing treatment after 30 cycles. It is generally known that the Li-ions intercalation in silicon electrodes can induce giant Si volume expansion, which leads to the cracked surface of silicon electrode and lose of electronic contacts of silicon nanoparticles. After the completion of 30 cycles, the coin cell was opened to investigate the morphology difference between the annealed and non-annealed electrodes. It is obvious that many interspaces appeared on the surface of non-annealed silicon anode. In comparison, the annealed electrode has much better the surface morphology. It reveals that the volume change of the annealed electrode is restrained effectively, which is beneficial to improve the electrochemical performance for silicon anode.

4. CONCLUSIONS

We have evaluated a one step annealing treatment of silicon-based electrodes and their thermal stability containing polyimide (PI) as a binder which showed drastic enhancement in the electrochemical performance of Si-based anode. The annealed electrodes achieved good surface morphology and control over silicon volume expansion to some extent. The electrode showed high initial charge reversible capacity of 1195.6 mAh g⁻¹, and good charge capacity retention of 93.6% for 30 cycles. In summary, the PI binder and annealing treatment improved the cycle performance of Si based anode for lithium ion batteries.

References

1. C. J. Wen and R. A. Huggins, *J Solid State Chem*, 37 (1981) 271
2. S. Pal, S. Damle, S. Patel, M. K. Dutta, P. N. Kumta and S. Maiti, *Battery Energy Technology*, 41

- (2012) 87
3. Y. Oumellal, N. Delpuech, D. Mazouzi, N. Dupré, J. Gaubicher, S. P. Moreau, B. Lestriez and D. Guyomard, *J Mater Chem*, 21 (2011) 6201
 4. C. K. Chan, H. Peng, G. Liu, K. McIlwrath, X. F. Zhang, R. A. Huggins and Y. Cui, *Nature Nanotechnology*, 3 (2007) 31
 5. M. Park, M. G. Kim, J. Joo, K. Kim, J. Kim, S. Ahn, Y. Cui and J. Cho, *Nano Lett*, 9 (2009) 3844
 6. W. Si, X. Sun, X. Liu, L. Xi, Y. Jia, C. Yan and O. G. Schmidt, *J Power Sources*, 267 (2014) 629
 7. X. Zhou, J. Tang, J. Yang, J. Xie and L. Ma, *Electrochim Acta*, 87 (2013) 663
 8. Y. Xu, G. Yin, Y. Ma, P. Zuo and X. Cheng, *J Mater Chem*, 20 (2010) 3216
 9. H. Tao, M. Huang, L. Fan and X. Qu, *Electrochim Acta*, 89 (2013) 394
 10. Q. Si, K. Hanai, T. Ichikawa, A. Hirano, N. Imanishi, Y. Takeda and O. Yamamoto, *J Power Sources*, 195 (2010) 1720
 11. M. Su, Z. Wang, H. Guo, X. Li, S. Huang, L. Gan and W. Xiao, *Powder Technol*, 249 (2013) 105
 12. A. Magasinski, B. Zdyrko, I. Kovalenko, B. Hertzberg, R. Burtovyy, C. F. Huebner, T. F. Fuller, I. Luzinov and G. Yushin, *ACS Applied Materials & Interfaces*, 2 (2010) 3004
 13. B. Koo, H. Kim, Y. Cho, K. T. Lee, N. Choi and J. Cho, *Angewandte Chemie International Edition*, 51 (2012) 8762
 14. N. Choi, K. H. Yew, W. Choi and S. Kim, *J Power Sources*, 177 (2008) 590
 15. S. Uchida, M. Mihashi, M. Yamagata, M. Ishikawa, *J. Power Sources*, 273 (2015) 118
 16. C. Wang, H. Wu, Z. Chen, M. T. McDowell, Y. Cui and Z. Bao, *Nature Chemistry*, 5 (2013) 1042
 17. J. S. Kim, W. Choi, K. Y. Cho, D. Byun, J. Lim and J. K. Lee, *J. Power Sources*, 244 (2013) 521
 18. N. Ding, J. Xu, Y. Yao, G. Wegner, I. Lieberwirth and C. Chen, *J Power Sources*, 192 (2009) 644
 19. K. Xu, *Chem Rev*, 104 (2004) 4303
 20. N. A. Kaskhedikar and J. Maier, *Adv Mater*, 21 (2009) 2664
 21. F. Maroni, R. Raccichini, A. Birrozzini, G. Carbonari, R. Tossici, F. Croce, R. Marassi and F. Nobili, *J Power Sources*, 269 (2014) 873
 22. W. Wang and P. N. Kumta, *ACS Nano*, 4 (2010) 2233
 23. X. Chen, X. Li, F. Ding, W. Xu, J. Xiao, Y. Cao, P. Meduri, J. Liu, G. L. Graff and J. G. Zhang, *Nano Lett*, 12 (2012) 4124
 24. L. Cui, R. Ruffo, C. K. Chan, H. Peng and Y. Cui, *Nano Lett*, 9 (2009) 491
 25. C. K. Chan, R. Ruffo, S. S. Hong, R. A. Huggins and Y. Cui, *J Power Sources*, 189 (2009) 34
 26. C. Delacourt, P. L. Ridgway, V. Srinivasan and V. Battaglia, *J Electrochem Soc.*, 161 (2014) A1253
 27. S. B. Gayathri, P. Kamaraj, M. Arthanareeswari and S. D. Kala, *Int. J. Electrochem. Sci.*, 9 (2014) 6113